Developmental Biology 505 (2024) 34–41

Contents lists available at ScienceDirect

Developmental Biology

journal homepage: www.elsevier.com/locate/developmentalbiology

# Small molecule-mediated reprogramming of *Xenopus* blastula stem cells to a neural crest state

Paul B. Huber [a,b], Carole LaBonne [a,b,*]

[a] Department of Molecular Biosciences, Northwestern University, Evanston, IL 60208, USA
[b] NSF-Simons Center for Quantitative Biology, Northwestern University, Evanston, IL 60208, USA

ARTICLE INFO

*Keywords:*
Wnt
BMP
Stem cell
Xenopus
Neural crest

ABSTRACT

Neural crest cells are a stem cell population unique to vertebrates that give rise to a diverse array of derivatives, including much of the peripheral nervous system, pigment cells, cartilage, mesenchyme, and bone. Acquisition of these cells drove the evolution of vertebrates and defects in their development underlies a broad set of neurocristopathies. Moreover, studies of neural crest can inform differentiation protocols for pluripotent stem cells and regenerative medicine applications. *Xenopus* embryos are an important system for studies of the neural crest and have provided numerous insights into the signals and transcription factors that control the formation and later lineage diversification of these stem cells. Pluripotent animal pole explants are a particularly powerful tool in this system as they can be cultured in simple salt solution and instructed to give rise to any cell type including the neural crest. Here we report a protocol for small molecule-mediated induction of the neural crest state from blastula stem cells and validate it using transcriptome analysis and grafting experiments. This is an powerful new tool for generating this important cell type that will facilitate future studies of neural crest development and mutations and variants linked to neurocristopathies.

## 1. Introduction

The evolutionary transition from simple chordate body plans to complex vertebrate body plans was driven by the acquisition of a novel stem cell population, the neural crest (Bronner and Le Douarin, 2012; Hall, 1999; Le Douarin and Kalcheim, 1999; Prasad et al., 2012). Neural crest cells display broad multi-germ layer potential. They contribute to ectodermal derivatives, including much of the peripheral nervous system, but also to many mesodermal cell types, including cartilage, bone, and smooth muscle, and also make contributions to otherwise endodermal organs such as the thyroid (Le Douarin and Kalcheim, 1999). Understanding the processes that govern establishment and maintenance of multipotency in the neural crest is of significant interest and importance to both developmental biology and regenerative medicine. Studies of the neural crest derive additional significance from both the central contribution of these cells to vertebrate evolution and the large number of congenital defects and cancers linked to defects in their development (Schock et al., 2023; York et al., 2020).

Investigations of the neural crest using embryos from *Xenopus* and other amphibians have yielded numerous important discoveries regarding the development of these cells, their role in sculpting the vertebrate body plan, and their links to human congenital disorders and diseases (Greenberg et al., 2019; LaBonne and Zorn, 2015; Piekarski et al., 2014; Schock and LaBonne, 2020). Indeed, it was studies in *Xenopus* that first demonstrated that pluripotent explants could be induced to a neural crest progenitor state by chordin-mediated BMP attenuation combined with Wnt/β-catenin signals (LaBonne and Bronner-Fraser, 1998a). That same study showed that Wnts could also induce neural crest in *Snai2* expressing explants, and subsequently transcription factor-mediated reprogramming was demonstrated using the neural plate border factors pax3 and zic1 (Hong and Saint-Jeannet, 2007; Sato et al., 2005). Reprogrammed explants using these methods have provided key insights into the neural crest gene regulatory network (GRN) (Pegoraro and Monsoro-Burq, 2013; Prasad et al., 2012; Schock et al., 2023).

There are, however, limitations to these reprogramming methods – all involve mRNA injections into early cleavage stage embryos followed by explanting the injected cells at blastula stages. mRNA injections lead to early expression of factors that might alter the developmental state of cells prematurely, potentially causing artifactual gene regulatory changes. Hormone-inducible transcription factors have been used to activate their function at the appropriate developmental time, however

* Corresponding author. Department of Molecular Biosciences, Northwestern University, Evanston, IL 60208, USA.
*E-mail address:* clabonne@northwestern.edu (C. LaBonne).

https://doi.org/10.1016/j.ydbio.2023.10.004
Received 28 September 2023; Received in revised form 13 October 2023; Accepted 16 October 2023
Available online 25 October 2023

transcription factors function cell autonomously and mRNA injection leads to heterogeneous expression levels across the injected tissue, making it impossible to generate explants with uniform cell states. We recently used *Xenopus* blastula explants to study the dynamic transcriptome changes that occur as initially pluripotent cells transit to four different lineage states (Johnson et al., 2022). This study intentionally initiated lineage instructions at the blastula stage to ensure that the pluripotent cells themselves had not been altered by earlier perturbations. Because the pluripotency and neural crest GRNs share many components (Buitrago-Delgado et al., 2015; Lavial et al., 2007; Lignell et al., 2017; Lukoseviciute et al., 2018; Scerbo and Monsoro-Burq, 2020; Schock et al., 2023; Zalc et al., 2021), it is arguably even more important when studying transit to this state to avoid perturbations that might have altered the state of the blastula stem cells. Here we describe a simple and novel protocol for small molecule-mediated induction of the neural crest state by modulating BMP/Wnt pathways that allows the state transition to be initiated only at blastula stages.

## 2. Results

### 2.1. Pharmacological induction of the neural crest state by modulating BMP/Wnt pathways

BMP and Wnt signaling pathways play central roles in the formation of the neural plate border and neural crest in all vertebrates in which it has been examined (García-Castro et al., 2002; LaBonne and Bronner-Fraser, 1998a; Lewis et al., 2004; Marchant et al., 1998; Mayor et al., 1995). In *Xenopus*, blastula explants can be re-programmed to a neural crest state by microinjection of mRNA encoding the BMP antagonist chordin and Wnt8 at the 2 cell stage (LaBonne and Bronner-Fraser, 1998a). To establish a protocol for uniformly inducing neural crest in these explants without relying on mRNA injection we utilized small molecules that function as inhibitors of BMP signaling and agonists of Wnt signaling.

K02288 is a highly selective 2-aminopyridine-based inhibitor of type 1 BMP receptors (Sanvitale et al., 2013). We have previously shown that K02288 (BMPi) is a potent BMP inhibitor that can induce a neural progenitor state in *Xenopus* blastula explants when treatment is initiated at blastula stages (Johnson et al., 2022). CHIR99021 (CHIR) is a potent pharmacological activator of the Wnt signaling pathway that works by inhibiting the active site of the kinase GSK3β, thereby stabilizing beta-catenin (Bennett et al., 2002; Ring et al., 2003). Blastula animal pole explants (stage 9 "animal caps") were treated with different concentrations of BMPi and CHIR and cultured to stage 17 when they were examined for neural crest and neural plate border markers by *in situ* hybridization (Fig. 1a). After testing numerous combinations of concentrations (data not shown), we found that treatment with 3 μM BMPi and 107 μM CHIR at 22 °C induced robust expression of the neural plate border marker, *pax3* [DMSO: 0/35 (0%), BMPi/CHIR: 24/24 (100%)] and the definitive neural crest marker, *snai2* [DMSO: 0/59 (0%), BMPi/CHIR: 82/82 (100%)] (Fig. 1b). During neural plate border formation *pax3* transcripts begin to accumulate during gastrulation and increase over time through neural plate stages (Session et al., 2016). To examine the timing of *pax3* expression in response to BMPi/CHIR treatment, we collected vehicle and drug-treated explants at stages 10.5, 11, 12, and 13 for *in situ* analysis. As with endogenous expression, *pax3*

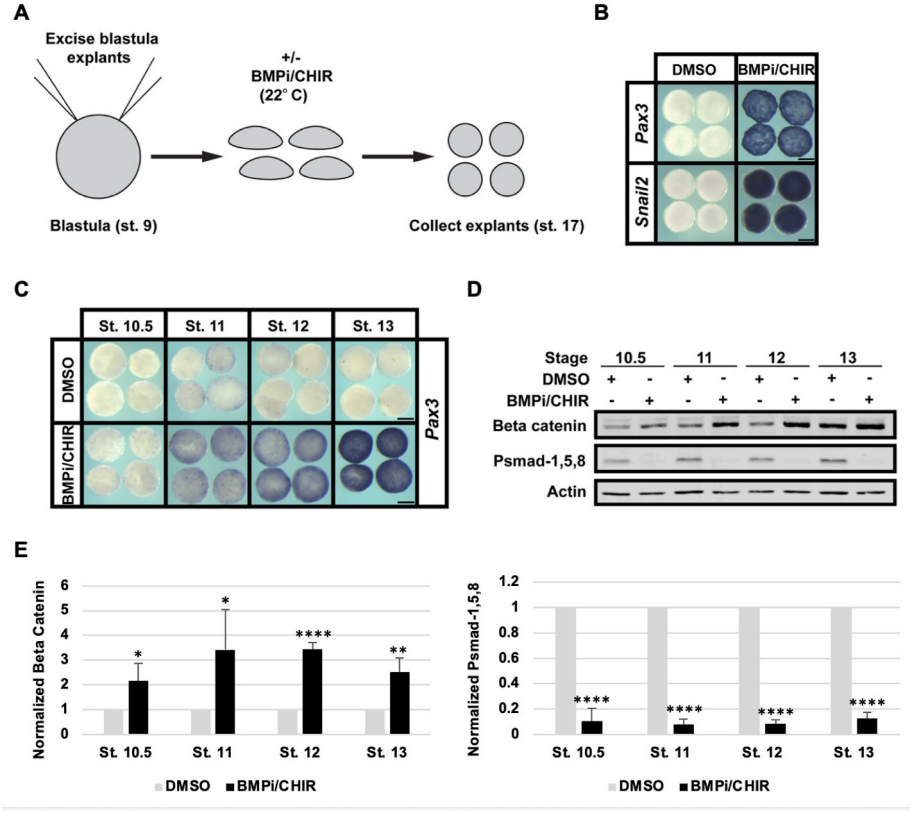


**Fig. 1.** Pharmacological induction of neural crest by modulating BMP/Wnt pathways. (A) Diagram outlining method for small molecule induction of the neural crest state from excised blastula explants. (B) *In situ* hybridization examining the expression of neural plate border and neural crest factors *pax3* and *snai2* in stage 17 explants following treatment with vehicle or 3 μM BMPi and 107 μM CHIR. (C) *In situ* hybridization examining the expression of *pax3* in vehicle or BMPi/CHIR-treated explants during gastrulation stages (10.5, 11, 12, 13). (D) Western blot for beta catenin, phospho-Smad-1,5,8, and actin with animal cap explants treated with vehicle or BMPi/CHIR, collected at the indicated stages. (E) Bar graphs showing the quantification of normalized beta catenin and phospho-Smad-1,5,8 levels (relative to actin) in western from part (D). For determining statistical significance, a standard one-tailed T-test with two sample equal variance was used. Asterisks denote significant p values (*$p \leq 0.05$, **$p \leq 0.01$, ***$p \leq 0.001$, ****$p \leq 0.0001$). Scale bars: 250 μm.

increased through stages 10.5 [DMSO: 0/23 (0%), BMPi/CHIR: 26/26 (100%)], 11 [DMSO: 0/23 (0%), BMPi/CHIR: 29/29 (100%)], and 12 [DMSO: 0/26 (0%), BMPi/CHIR: 34/34 (100%)] with the most robust expression noted at stage 13 [DMSO: 0/24 (0%), BMPi/CHIR: 25/25 (100%)] (Fig. 1c).

Having established concentrations of BMPi and CHIR that robustly induced expression of neural plate border and neural crest markers we wished to directly evaluate the effects of this treatment on BMP and Wnt signaling. BMP pathway activity can be assessed by Western blot analysis using antibodies that detect phosphorylated BMP R-smads (pSmad-1/5/8). Similarly, Wnt signaling can be assessed by examining β-catenin levels, which increase in response to Wnt activity. Explants treated with vehicle or with BMPi/CHIR were collected at stages 10.5, 11, 12, and 13 for Western analysis (10 explants per condition with three biological replicates). BMPi/CHIR treatment led to a reduction of pSmad-1/5/8 levels and an increase in β-catenin levels at all stages (Fig. 1d). Quantification showed that β-catenin levels increased between 2 and 3-fold across these stages, while pSmad-1/5/8 was consistently reduced by over 80% (Fig. 1e).

### 2.2. Transcriptome analysis of BMPi/CHIR-induced neural crest

We next wished to compare the transcriptomes of neural crest generated by BMPi/CHIR to that of neural crest generated by injection of mRNA encoding Wnt8 and Chordin. RNA was isolated from stage 17 explants that had been treated at stage 9 with vehicle or BMPi/CHIR (10 explants per condition across 3 replicates) and used to generate Illumina libraries for sequencing. We used differential expression analysis (DESeq2) to quantify the gene expression differences in vehicle vs BMPi/CHIR treated explants and compared them to transcriptomes from stage 17 control (epidermal) or Wnt/chordin-injected neural crest explants (Huber et al., in revision). We found that relative to control samples, the induced levels of key neural plate border (*pax3*, *zic1*) and neural crest (*foxd3*, *sox10*, *snai1*, *snai2*) genes were highly similar with the main difference being a more robust induction of *zic1* when neural crest was induced by BMPi/CHIR (Fig. 2a; padj $< 1 \times 10^{-12}$ for all genes). This suggests that a comparable neural crest state is generated by both induction methods.

We next used principal component analysis (PCA) to compare the transcriptomes of BMPi/CHIR-induced neural crest, Wnt/chordin-induced neural crest, and a published data set generated from neural folds dissected from stage 17 embryos (Plouhinec et al., 2017). PC1 accounts for 80% of the variance in these data sets and the uninjected control and vehicle-treated explants clustered together and distant from all three neural crest data sets along this axis in keeping with their epidermal nature (Fig. 2b). The BMPi/CHIR- and Wnt/chordin-induced neural crest data sets clustered with respect to both principal components. Interestingly, the dissected neural folds did not cluster with the neural crest induced explants, with the variance being explained by PC2 (12%). A heatmap of the top 30 genes contributing to the variance between all data sets shows that all three neural crest transcriptomes show upregulation of the neural plate border and neural crest genes *pax3*, *foxd3*, *sox10* relative to the epidermal controls. The dissected neural folds also express genes such as *en2*, *alx4*, *nhlh1* and *neurod1* that are expressed in the developing central nervous system at stage 17 (Bury et al., 2008; Chang and Harland, 2007; Green and Vetter, 2011; Liu and Harland, 2005; Takahashi et al., 1998) and drive the variance in PC2. Together these analyses indicate that BMPi/CHIR treatment at stage 9 generates a neural crest state as effectively as does injection of mRNA encoding Wnt8/chordin at the 2-cell stage, and is a better representation of the neural crest state than dissected neural folds. Importantly, generating neural crest via BMPi/CHIR treatment at stage 9 initiates the state transition from wild-type pluripotent blastula cells. By contrast, when neural crest is generated by injection of Wnt8/chordin mRNA at the 2-cell stage, significant gene expression differences have already occurred by the blastula stage (Table 1), including up-regulation of

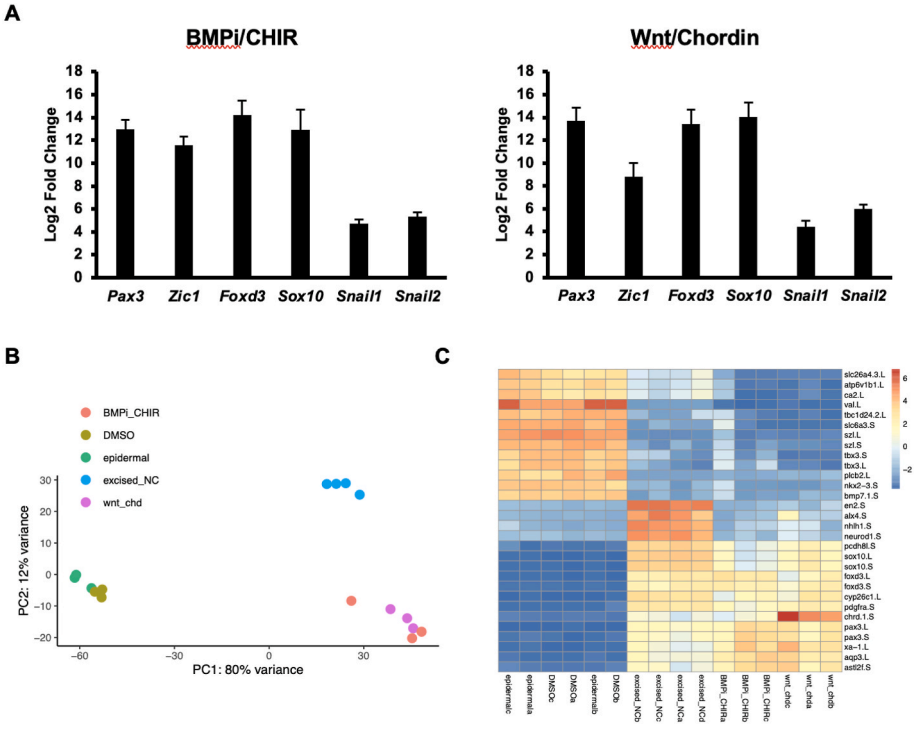


**Fig. 2.** Transcriptome analysis of BMPi/CHIR-induced neural crest. (A) Bar graphs depicting log2 fold change determined by DEseq2 for neural plate border (*pax3*, *zic1*) and neural crest (*foxd3*, *sox10*, *snai1*, *snai2*) genes in BMPi/CHIR- and wnt/chordin-induced explants versus controls. Error bars represent the standard error of log2 fold change. (B) PCA plot comparing the variance between the transcriptomes of epidermal (DMSO, epidermal) and neural crest (BMPi/CHIR, wnt_chd, excised_NC) explants. All explants were collected at stage 17. (C) Heatmaps of the top 30 genes contributing to the variance between the cell populations compared in the PCA plot in part (B).

**Table 1**
Genes overexpressed in wnt/chordin-induced neural crest explants. List of genes overexpressed (log2 fold change >1.5, p ≤ 0.05) in stage 9 explants from embryos injected at the 2 cell stage with wnt8 and chordin mRNAs. Differential gene expression was determined by DEseq2 after sequencing total RNA isolated from control and induced explants.

| gene | log2FoldChange | padj |
|---|---|---|
| chrd.1.S | 16.562942 | 4.67E−47 |
| hbg1.L | 15.52012104 | 8.37E−35 |
| wnt8a.L | 14.15900664 | 4.30E−265 |
| wnt8a.S | 13.39035992 | 6.32E−25 |
| chrd.1.L | 9.813824608 | 7.15E−06 |
| sia 1.L | 9.719608316 | 3.73E−11 |
| nodal 3.2.L | 9.227948498 | 0.00025711 |
| LOC108710651 | 6.629421685 | 1.67E−27 |
| LOC108703460 | 6.329563273 | 8.54E−28 |
| sp5.L | 5.183499795 | 0.00480296 |
| foxa4.L | 5.033986063 | 0.00029132 |
| sia 2.S | 4.308081132 | 0.00151462 |
| admp.S | 3.915123154 | 9.27E−06 |
| admp.L | 3.408428671 | 8.86E−05 |
| sp5l.S | 1.965537762 | 0.01580687 |
| rasl11 b.L | 1.78468059 | 0.00625916 |

*nodal*, *siamois* and *admp* which all have known roles in patterning and cell fate decisions in early embryos.

### 2.3. BMPi/CHIR-induced neural crest cells migrate and display a cadherin switch

Following neurulation, neural crest cells undergo an epithelial-to-mesenchymal transition (EMT), and migrate extensively throughout the embryo (Schock et al., 2023). To determine if BMPi/CHIR-induced neural crest possess the capacity to undergo EMT and migrate we carried out grafting experiments (LaBonne and Bronner-Fraser, 2000). eGFP-labelled explants were treated with BMPi/CHIR or vehicle at stage 9 and cultured to stage 17. Explants were then grafted into non-labelled host embryos from which the neural fold had been removed unilaterally (Fig. 3a). Cells from vehicle treated explants remained dorsally localized near the graft site and did not display migratory behavior (n = 20, 0% migration). By contrast, most cells from BMPi/CHIR-induced explants migrated extensively in mandibular, hyoid and branchial streams with the timing of endogenous neural crest cells (n = 27, 100% migration). This demonstrates BMPi/CHIR-induced neural crest recapitulates the migratory behaviors of endogenous neural crest (Fig. 3b).

To confirm that post-migratory BMPi/CHIR-induced neural crest cells display appropriate gene expression we examined expression of Sox9 protein in stage 30 embryos via immunofluorescence. Endogenously, cartilage forming neural crest cells express Sox9 as they populate the pharyngeal arches. In embryos receiving grafts of vehicle treated cells there are no GFP(+) cells that express Sox9. Sox9-expressing cells are notably absent in pharyngeal pouches as the endogenous neural crest had been ablated (Fig. 3c; n = 13, 0% in pharyngeal pouches). Instead, GFP(+) cells from vehicle treated grafts remained dorsally localized at the graft site. By contrast, embryos receiving grafts of BMPi/CHIR-induced neural crest displayed appropriate patterned GFP(+)/Sox9(+) cells that had migrated to and populated the pharyngeal pouches (n = 14, 100% in pharyngeal arches). Endogenously, migrating neural crest cells undergo a switch from expressing E-cadherin (cdh1) to N-cadherin (cdh2) (Scarpa et al., 2015). Consistent with this we found that BMPi/CHIR-induced neural crest explants also display this switch in cadherin expression (Fig. 3d; padj $< 1 \times 10^{-15}$ for all genes).

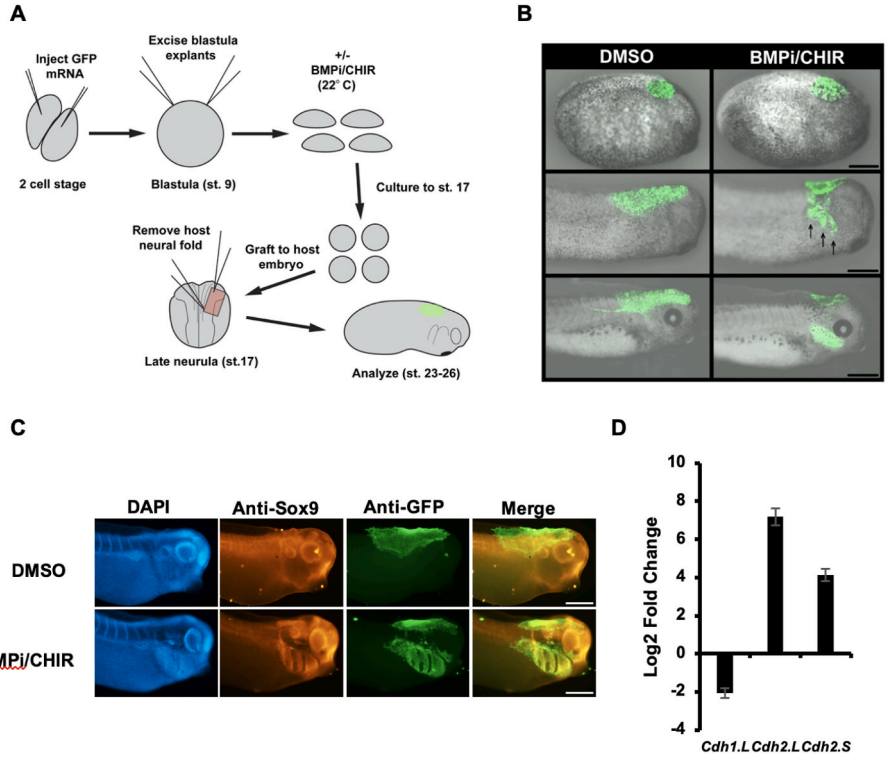


**Fig. 3.** BMPi/CHIR-induced neural crest cells migrate and display a cadherin switch. (A) Diagram of experimental design to test the ability of BMPi/CHIR-treated explants to function like endogenous neural crest when grafted into host sibling embryos. (B) Live images of GFP in grafted embryos, immediately after grafting (stage 17) and at stages 23 and 41. Arrowheads denote migrating cells. (C) Images depicting immunofluorescence of fixed stage 30 embryos grafted with DMSO or BMPi/CHIR-treated explants. DAPI staining was used along with antibodies probing for both Sox9 and GFP. (D) Bar graph depicting log2 fold change determined by DEseq2 of BMPi/CHIR-treated explants (stage 17) compared to controls for e-cadherin (*cdh1.L*) and n-cadherin (*cdh2.L/S*) genes. Error bars represent the standard error of log fold change. Scale bars: 500 μm.

### 2.4. BMPi/CHIR-induced neural crest cells differentiate into multiple neural crest derivatives

Following their migration, neural crest cells give rise to a large and diverse set of derivatives (Prasad et al., 2012; Mayor and Theveneau, 2013). These cell types include neurons and glia of the sensory, sympathetic, and parasympathetic nervous systems, pigment-producing cells in the epidermis (melanocytes), and much of the connective tissue and skeletal structures that form the vertebrate head (LaBonne and Bronner-Fraser, 1998b; York and McCauley, 2020). We therefore examined if BMPi/CHIR induced neural crest cells would give rise to appropriate derivatives following their migration *in vivo*. To test this, we cultured embryos grafted with GFP(+) BMPi/CHIR-induced neural crest cells to later tadpole stages (approximately stage 46). In tadpoles that received grafts of vehicle treated cells that showed no migratory ability, GFP(+) cells remained in the dorsal epidermis and no incorporation of those cells into neural crest derived cell types was observed (n = 18, 100%) (Fig. 4a). By contrast, tadpoles that received grafts of BMPi/CHIR-induced neural crest cells displayed GFP(+) cells throughout the cartilage on the grafted side of the animal, indicating that those cells had differentiated into neural crest-derived chondrocytes with normal morphologies (n = 27, 100%). In addition, tadpoles that received grafts of BMPi/CHIR-induced neural crest cells labelled with nuclear H2B:GFP displayed GFP(+) cells that had differentiated into melanocytes (Fig. 4b; n = 5, 100%). Similarly, BMPi/CHIR-induced explants cultured to stage 27 displayed numerous cells expressing *mitf*, a marker for melanocyte differentiation, as visualized by hybridized chain reaction (HCR) RNA-FISH (Choi et al., 2014) of stage 27 [DMSO: 0/16 (0%), BMPi/CHIR: 13/16 (81.3%)]. Finally, immunofluorescence in stage 46 tadpoles for HuCD (*elval3/4*), which marks pan-neuronal cells, revealed GFP(+) cells in the tri-geminal ganglia but not in the brain or other non-neural crest-derived neural tissues, demonstrating that BMPi/CHIR-neural crest cells can differentiate into neurons, in addition to chondrocytes and melanocytes. Collectively these data demonstrate that BMPi/CHIR treatment of pluripotent blastula cells is a simple and highly effective method for generating neural crest cells that migrate and differentiate like endogenous neural crest.

## 3. Discussion

A large set of neurocristopathies, diseases, syndromes and congenital malformations have been identified that are linked to defects in the formation, migration, and/or differentiation neural crest cells. These include ciliopathies, ribosomopathies, epigenetic defects and cancers (Cerrizuela et al., 2020; McGonigle and Ruggeri, 2014; Vega-Lopez et al., 2018). Studies of the neural crest are thus of high clinical significance. Moreover, acquisition of neural crest stem cells played a central role in the evolution of vertebrates and this too is an important area of investigation. Decades of work in *Xenopus* have made invaluable contributions to our understanding of normal neural crest development (Groves and LaBonne, 2014; Prasad et al., 2012; Schock et al., 2023). Increasingly this system has also proven to be a powerful platform for investigation of mutations and variants linked to neurocristopathies (Bajpai et al., 2010; Greenberg et al., 2019; Lasser et al., 2022; Mills et al., 2019; Park et al., 2022; Schwenty-Lara et al., 2020; Shah et al., 2020; Timberlake et al., 2021; Wyatt et al., 2020).

Here we develop and validate a protocol for small molecule-mediated induction of neural crest cells from blastula explants using the BMP inhibitor K02288 (BMPi) and the GSK3 inhibitor CHIR (An et al., 2014; Sanvitale et al., 2013). We show using both *in situ* hybridization and transcriptome analysis that these cells have a neural crest gene regulatory signature. Furthermore, these cells behaved like endogenous neural crest when transplanted into the neural folds of host embryos. BMPi/CHIR induced cells were found to migrate appropriately and give rise to a range of neural crest derivatives, including chondrocytes, melanocytes, and neurons in cranial ganglia. This method provides a powerful and efficient experimental platform for investigating neural crest biology to a wide range of research programs.

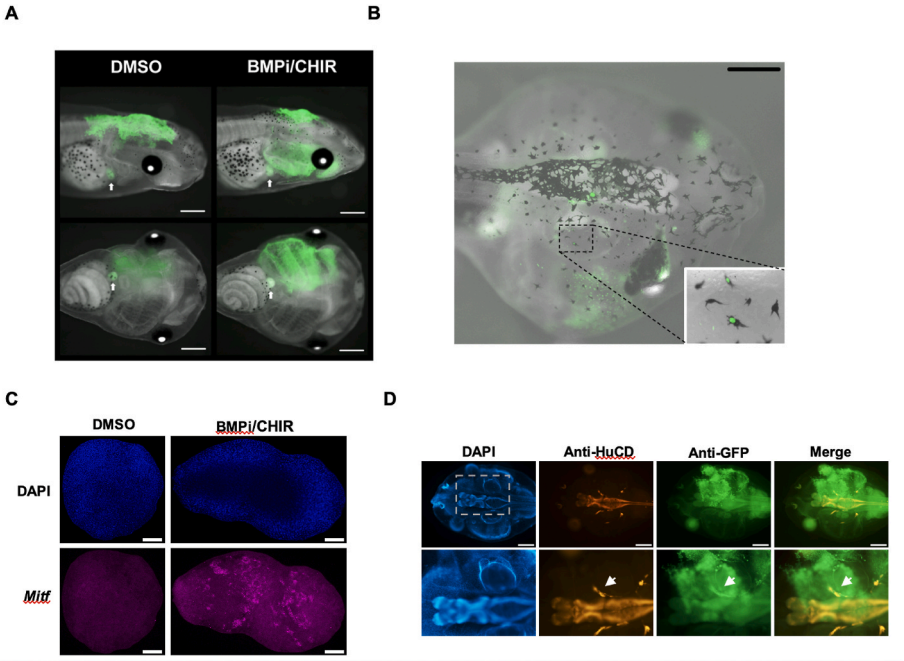


**Fig. 4.** BMPi/CHIR-induced neural crest cells differentiate into multiple neural crest derivatives. (A) Live images of eGFP in stage 46 embryos grafted with DMSO or BMPi/CHIR-treated explants. White arrowheads denote autofluorescence in the gallbladder. Scale bars: 500 μm (B) Live image of H2B:GFP in stage 46 embryo grafted with BMPi/CHIR-treated explants with inset of individual melanocytes containing nuclear GFP. Scale bars: 500 μm (C) HCR of stage 27 animal caps treated with DMSO or BMPi/CHIR, probed for *mitf*. Scale bars: 100 μm (D) Images depicting immunofluorescence of fixed stage 46 embryos grafted with BMPi/CHIR-treated explants. DAPI staining was used along with antibodies probing for both HuCD and GFP. Bottom panels show inset labelled in top left corner for all channels, white arrowheads indicate areas of overlap of HuCD and GFP expression in neuronal ganglia. Scale bars: 500 μm.

Due to the large number of embryos that can be obtained from a single mating, *Xenopus* is ideal for studies requiring significant amounts of tissue for genomics and proteomics (Chung et al., 2014; Onjiko et al., 2015; Wühr et al., 2014; Yanai et al., 2011). The large size and rapid external development of these embryos are also significant experimental advantages as is the ease of grafting and explant culture in this system. Explants of pluripotent cells from blastula stage embryos (sometimes called "animal caps") have proven particularly valuable for elucidating the signals and regulatory processes that underlie the formation of a myriad of cell types and organs during development (Ariizumi et al., 2009, 2017; Buitrago-Delgado et al., 2018; Borchers and Pieler, 2010; Geary and LaBonne, 2018; Johnson et al., 2022; Rao and LaBonne, 2018).

Using these pluripotent explants it has been shown that the neural crest state can be induced by combinations of signaling pathways (Wnt/BMP) or transcription factors (pax3/zic1, snai2) (Gomez et al., 2019; LaBonne and Bronner-Fraser, 1998a; Leung et al., 2016; Milet et al., 2013). The advantage of these explants is that they allow for investigation of neural crest cells over time *ex vivo* where their environment and signaling cues can be precisely controlled. While explants of endogenous neural crest have also been used for such studies, one downside of this approach is that it is nearly impossible to avoid contamination with epidermal and CNS cells which can confound experimental outcomes and genomic analyses as highlighted by our study (Fig. 2b and c).

Historically one limitation of generating neural crest from blastula explants has been that their reprograming was mostly achieved via micro-injection of mRNA at the 2-cell stage. A concern was that this might alter the developmental state of those cells potentially leading to artifactual gene regulatory changes. Our results here show that is indeed the case. We find that explants previously injected with mRNA encoding Wnt8 and chordin at the 2-cell stage display significant upregulation of developmentally important genes at stage 9 relative to control explants, including *nodal*, *admp*, *siamois*, and *sp5* (Table 1). While hormone-inducible transcription factors can be used to activate reprogramming at an appropriate developmental time, their expression is heterogeneous across the explants which also can affect developmental states.

Moving forward this protocol will facilitate a number of areas of investigation. We recently used animal pole explants to quantitatively follow the dynamic transcriptome changes that occur as initially pluripotent cells transit to four different lineage states (Johnson et al., 2022). Using CHIR/BMPi-mediated induction, it will be possible to build on those data by studying the establishment of neural crest stem cells with high temporal resolution using RNAseq, scRNAseq and ATACseq. In addition to *ex vivo* studies grafting experiments will also enable the development and behavior of an initially homogeneous population of labelled induced neural crest cells to be studied at single cell resolution. Finally, this method provides a new tool for dissecting the gene regulatory architecture underlying the development and evolution of neural crest cells, for elucidating methods for further directing the formation of specific neural crest derivatives, and for investigating mutations and variants linked to neurocristopathies.

## 4. Materials and methods

### 4.1. Embryological methods

Wild type *Xenopus laevis* embryos were staged and collected according to standard methods (Nieuwkoop and Faber, 1994). *In situ* hybridizations of explanted animal caps were performed using previously described methods (LaBonne and Bronner-Fraser, 1998a,b). Microinjection of Wnt8a/chordin, eGFP, and H2B-GFP mRNAs (Ambion, mMessage mMachine SP6 Transcription Kit) was done in both cells of 2-cell stage embryos as previously described (Lee et al., 2012). Injected embryos were cultured in 0.1× Marc's Modified Ringer's Solution (MMR) [0.1 M NaCl, 2 mM KCl, 1 mM $MgSO_4$, 2 mM $CaCl_2$, 5 mM HEPES (pH 7.8), 0.1 mM EDTA] until being dissected for animal cap explant assays. Animal cap explants were manually dissected during the late blastula stage and cultured in 1xMMR. Drug-treated explants [3 μM K02288, 107 μM CHIR99021 (Sigma-Aldrich)] were cultured at 22 °C from late stage 9 until the indicated collection times. All manipulated explants were fixed in 1× MEM [100 mM MOPS (pH 7.4), 2 mM EDTA, 1 mM $MgSO_4$] with 4% formaldehyde and dehydrated in methanol prior to *in situ* hybridization assays, or used for WB analysis, RNA extraction, HCR or grafting assays. Results shown are representative of a minimum of three biological replicates.

### 4.2. Western blot analysis

For Western blot analysis, 10 animal explants per condition were lysed in TNE lysis buffer [50 mM Tris-HCl (pH 7.4), 150 mM NaCl, 0.5 mM EDTA, and 0.5% Triton X-100] supplemented with protease inhibitors [Aprotinin, Leupeptin and phenylmethylsulfonyl fluoride (PMSF)] and a complete Mini tablet (Roche). Proteins were resolved by SDS-PAGE, blotted, and then probed for using the following antibodies: anti-beta catenin (sc7963, Santa Cruz, 1:200), anti-phospho-Rsmad-1/5/8 (Ser 463/465, Sigma-Aldrich, 1:1000), and anti-actin (A2066, Sigma-Aldritch, 1:5000). IRDye secondary antibodies were then used to detect proteins using the Odyssey platform (LI-COR Biosciences). Protein amounts were quantified using the Image Studio Lite software (LI-COR Biosciences), using actin for normalization of relative beta catenin and phospho-Rsmad-1/5/8 levels.

### 4.3. RNA isolation, library prep, RNAseq and computational analyses

Isolation of total RNA was performed by extraction from 10 animal explants with TRIZOL reagent and LiCl precipitation. 500 ng of RNA was used for library prep with the TruSeq library prep kit (Illumina) and was sequenced using Next Seq 500 Sequencing. Obtained reads were checked for quality by FAST-QC (Babraham Bioinformatics), then aligned to the *Xenopus laevis* genome 9.2 (Xenbase) using STAR aligner (Dobin et al., 2013). Aligned reads were counted using HTSeq Counts (Anders et al., 2015). Rstudio was used to do PCA and differential expression analysis with the DESeq2 package, applying a minimum raw read count of 15 counts with significance defined as $p_{adj} < 0.05$ (Love et al., 2014). For previously published RNAseq data sets [stage 17 Wnt/Chordin-injected explants with control (Huber et al., in revision) and dissected neural crest (Plouhinec et al., 2017)], FASTQ files were downloaded from the European Nucleotide Archive (https://www.ebi.ac.uk/ena/browser/home) and processed in the same manner as the transcriptomic data set generated in this study.

### 4.4. Grafting, immunofluorescence, and HCR

For grafting experiments, either eGFP or H2b-GFP mRNA was used as a lineage tracer for migratory and post-migratory cranial NC cells. The cranial NC was removed with forceps from host embryos at stage 16/17, and immediately replaced with same stage drug treated or vehicle treated explants which were opened and flattened with hair loop knife. A very small piece of coverslip was carefully placed over grafted embryos for 20 min to allow the explant to heal, then the embryos were each individually moved into a well of a 12 well plate coated with 1% agarose containing 1xMMR plus gentamycin. Embryos were imaged through stages 18–46 to assess migratory ability and incorporation of GFP(+) cells into NC derivatives. Tadpoles were imaged live after being anesthetized with 0.05% tricaine mesylate (MS-222) in 0.1xMMR solution or fixed in 1xMEM with 4% formaldehyde and moved to methanol before performing immunofluorescence (IF). The following antibodies were used for IF: anti-Sox9 (AB5535, Sigma, 1:500), anti-GFP (A10262, Invitrogen, 1:500), and anti-HuCD (A210554, Abcam, 1:500). HCR (hybridized chain reaction) was performed on stage 27 explants as previously described (Ibarra-García-Padilla et al., 2021). *mitf* probe and

amplifiers were obtained from Molecular Instruments, Inc. (https://www.molecularinstruments.com/).

### 4.5. Animals

All animal procedures were approved by the Institutional Animal Care and Use Committee, Northwestern University, and are in accordance with the National Institutes of Health's Guide for the Care and Use of Laboratory Animals.

## Declaration of competing interest

The authors declare that they have no known competing financial interests or personal relationships that could have appeared to influence the work reported in this paper.

**Acknowledgements**

We thank members of the LaBonne laboratory for helpful discussions. This work was supported by grants from the Simons Foundation (597491-RWC) the National Science Foundation (1764421) and the NIH (R01GM116538).

## Data availability

Data has been made available on GEO (GSE230350).

## Appendix A. Supplementary data

Supplementary data to this article can be found online at https://doi.org/10.1016/j.ydbio.2023.10.004.

## References

An, W.F., Germain, A.R., Bishop, J.A., Nag, P.P., Metkar, S., Ketterman, J., Walk, M., Weiwer, M., Liu, X., Patnaik, D., 2014. Discovery of Potent and Highly Selective Inhibitors of GSK3b. Probe Reports from the NIH Molecular Libraries Program. National Center for Biotechnology Information (US), 2010. PMID: 23658955.

Anders, S., Pyl, P.T., Huber, W., 2015. HTSeq—a Python framework to work with high-throughput sequencing data. Bioinformatics 31, 166–169.

Ariizumi, T., Michiue, T., Asashima, M., 2017. In vitro induction of Xenopus embryonic organs using animal cap cells. Cold Spring Harb. Protoc. 2017 (12), prot097410.

Ariizumi, T., Takahashi, S., Chan, T.c., Ito, Y., Michiue, T., Asashima, M., 2009. Isolation and differentiation of Xenopus animal cap cells. Curr. Protocols Stem Cell Biol. 9, 1D. 5.1-1D. 5.31.

Bajpai, R., Chen, D.A., Rada-Iglesias, A., Zhang, J., Xiong, Y., Helms, J., Chang, C.-P., Zhao, Y., Swigut, T., Wysocka, J., 2010. CHD7 cooperates with PBAF to control multipotent neural crest formation. Nature 463, 958–962.

Bennett, C.N., Ross, S.E., Longo, K.A., Bajnok, L., Hemati, N., Johnson, K.W., Harrison, S. D., MacDougald, O.A., 2002. Regulation of Wnt signaling during adipogenesis. J. Biol. Chem. 277, 30998–31004.

Borchers, A., Pieler, T., 2010. Programming pluripotent precursor cells derived from Xenopus embryos to generate specific tissues and organs. Genes 1, 413–426.

Bronner, M.E., Ledouarin, N.M., 2012. Development and evolution of the neural crest: an overview. Dev. Biol. 366, 2–9.

Buitrago-Delgado, E., Nordin, K., Rao, A., Geary, L., LaBonne, C., 2015. Shared regulatory programs suggest retention of blastula-stage potential in neural crest cells. Science 348, 1332–1335.

Buitrago-Delgado, E., Schock, E.N., Nordin, K., LaBonne, C., 2018. A transition from SoxB1 to SoxE transcription factors is essential for progression from pluripotent blastula cells to neural crest cells. Dev. Biol. 444, 50–61.

Bury, F.J., Moers, V., Yan, J., Souopgui, J., Quan, X.J., De Geest, N., Kricha, S., Hassan, B. A., Bellefroid, E.J., 2008. Xenopus BTBD6 and its Drosophila homologue lute are required for neuronal development. Dev. Dyn. 237, 3352–3360.

Cerrizuela, S., Vega-Lopez, G.A., Aybar, M.J., 2020. The role of teratogens in neural crest development. Birth Defects Res. 112, 584–632.

Chang, C., Harland, R.M., 2007. Neural induction requires continued suppression of both Smad 1 and Smad 2 signals during gastrulation. Development 134 (21), 3861–3872.

Choi, H.M., Beck, V.A., Pierce, N.A., 2014. Next-generation in situ hybridization chain reaction: higher gain, lower cost, greater durability. ACS Nano 8, 4284–4294.

Chung, M.-I., Kwon, T., Tu, F., Brooks, E.R., Gupta, R., Meyer, M., Baker, J.C., Marcotte, E.M., Wallingford, J.B., 2014. Coordinated genomic control of ciliogenesis and cell movement by RFX2. Elife 3, e01439.

Dobin, A., Davis, C.A., Schlesinger, F., Drenkow, J., Zaleski, C., Jha, S., Batut, P., Chaisson, M., Gingeras, T.R., 2013. STAR: ultrafast universal RNA-seq aligner. Bioinformatics 29, 15–21.

García-Castro, M.n.I., Marcelle, C., Bronner-Fraser, M., 2002. Ectodermal Wnt function as a neural crest inducer. Science 297, 848–851.

Geary L, LaBonne C., 2018. FGF mediated MAPK and PI3K/Akt Signals make distinct contributions to pluripotency and the establishment of Neural Crest. Elife. 19;7: e33845. doi: 10.7554/eLife.33845.

Gomez, G.A., Prasad, M.S., Sandhu, N., Shelar, P.B., Leung, A.W., García-Castro, M.I., 2019. Human neural crest induction by temporal modulation of WNT activation. Dev. Biol. 449 (2), 99–106.

Green, Y.S., Vetter, M.L., 2011. EBF factors drive expression of multiple classes of target genes governing neuronal development. Neural Dev. 6, 1–18.

Greenberg, R.S., Long, H.K., Swigut, T., Wysocka, J., 2019. Single amino acid change underlies distinct roles of H2A. Z subtypes in human syndrome. Cell 178, 1421–1436.

Groves, A.K., LaBonne, C., 2014. Setting appropriate boundaries: fate, patterning and competence at the neural plate border. Dev. Biol. 389, 2–12.

Hall, B., 1999. The Neural Crest in Development and Evolution. Springer Verlag.

Hong, C.-S., Saint-Jeannet, J.-P., 2007. The activity of Pax3 and Zic1 regulates three distinct cell fates at the neural plate border. Mol. Biol. Cell 18, 2192–2202.

Huber, P., Rao, A., LaBonne, C., 2023. BET Activity Plays an Essential Role in Control of Stem Cell Attributes in *Xenopus*. Development (in revision).

Ibarra-García-Padilla, R., Howard IV, A.G.A., Singleton, E.W., Uribe, R.A., 2021. A protocol for whole-mount immuno-coupled hybridization chain reaction (WICHCR) in zebrafish embryos and larvae. STAR Protocols 2, 100709.

Johnson, K., Freedman, S., Braun, R., LaBonne, C., 2022. Quantitative analysis of transcriptome dynamics provides novel insights into developmental state transitions. BMC Genom. 23, 723.

LaBonne, C., Bronner-Fraser, M., 1998a. Neural crest induction in Xenopus: evidence for a two-signal model. Development 125, 2403–2414.

LaBonne, C., Bronner-Fraser, M., 2000. Snail-related transcriptional repressors are required in Xenopus for both the induction of the neural crest and its subsequent migration. Dev. Biol. 221, 195–205.

LaBonne, C., Bronner-Fraser, M., 1998b. Induction and patterning of the neural crest, a stem cell-like precursor population. J. Neurobiol. 36, 175–189.

LaBonne, C., Zorn, A.M., 2015. Modeling human development and disease in Xenopus. Dev. Biol. 408, 179.

Lasser, M., Bolduc, J., Murphy, L., O'Brien, C., Lee, S., Girirajan, S., Lowery, L.A., 2022. 16p12. 1 deletion orthologs are expressed in motile neural crest cells and are important for regulating craniofacial development in Xenopus laevis. Front. Genet. 13, 833083.

Lavial, F., Acloque, H., Bertocchini, F., MacLeod, D.J., Boast, S., Bachelard, E., Montillet, G., Thenot, S., Sang, H.M., Stern, C.D., 2007. The Oct 4 homologue PouV and Nanog regulate pluripotency in chicken embryonic stem cells. Development 134 (19), 3549–3563.

Le Douarin, N., Kalcheim, C., 1999. The Neural Crest, second ed. Cambridge University Press, New York.

Lee, P.-C., Taylor-Jaffe, K.M., Nordin, K.M., Prasad, M.S., Lander, R.M., LaBonne, C., 2012. SUMOylated SoxE factors recruit Grg4 and function as transcriptional repressors in the neural crest. J. Cell Biol. 198, 799–813.

Leung, A.W., Murdoch, B., Salem, A.F., Prasad, M.S., Gomez, G.A., García-Castro, M.I., 2016. WNT/β-catenin signaling mediates human neural crest induction via a pre-neural border intermediate. Development 143, 398–410.

Lewis, J.L., Bonner, J., Modrell, M., Ragland, J.W., Moon, R.T., Dorsky, R.I., Raible, D. W., 2004. Reiterated Wnt signaling during zebrafish neural crest development. Development 131 (6), 1299–1308.

Lignell, A., Kerosuo, L., Streichan, S.J., Cai, L., Bronner, M.E., 2017. Identification of a neural crest stem cell niche by Spatial Genomic Analysis. Nat. Commun. 8, 1–11.

Liu, K.J., Harland, R.M., 2005. Inhibition of neurogenesis by SRp38, a neuroD-regulated RNA-binding protein. Development 132 (7), 1511–1523.

Love, M.I., Huber, W., Anders, S., 2014. Moderated estimation of fold change and dispersion for RNA-seq data with DESeq2. Genome Biol. 15, 1–21.

Lukoseviciute, M., Gavriouchkina, D., Williams, R.M., Hochgreb-Hagele, T., Senanayake, U., Chong-Morrison, V., Thongjuea, S., Repapi, E., Mead, A., Sauka-Spengler, T., 2018. From pioneer to repressor: bimodal foxd3 activity dynamically remodels neural crest regulatory landscape in vivo. Dev. Cell 47, 608–628 e606.

Marchant, L., Linker, C., Ruiz, P., Guerrero, N., Mayor, R., 1998. The inductive properties of mesoderm suggest that the neural crest cells are specified by a BMP gradient. Dev. Biol. 198, 319–329.

Mayor, R., Morgan, R., Sargent, M.G., 1995. Induction of the prospective neural crest of Xenopus. Development 121, 767–777.

Mayor, R., Theveneau, E., 2013. The neural crest. Development 140, 2247–2251.

McGonigle, P., Ruggeri, B., 2014. Animal models of human disease: challenges in enabling translation. Biochem. Pharmacol. 87, 162–171.

Milet, C., Maczkowiak, F., Roche, D.D., Monsoro-Burq, A.H., 2013. Pax3 and Zic1 drive induction and differentiation of multipotent, migratory, and functional neural crest in Xenopus embryos. Proc. Natl. Acad. Sci. U. S. A. 110, 5528–5533.

Mills, A., Bearce, E., Cella, R., Kim, S.W., Selig, M., Lee, S., Lowery, L.A., 2019. Wolf-Hirschhorn Syndrome-associated genes are enriched in motile neural crest cells and affect craniofacial development in Xenopus laevis. Front. Physiol. 10, 431.

Nieuwkoop, P.D., Faber, J., 1994. Normal table of Xenopus laevis (Daudin) : a systematical and chronological survey of the development from the fertilized egg till the end of metamorphosis. Garland Pub, New York.

Onjiko, R.M., Moody, S.A., Nemes, P., 2015. Single-cell mass spectrometry reveals small molecules that affect cell fates in the 16-cell embryo. Proc. Natl. Acad. Sci. U. S. A. 112, 6545–6550.

Park, B.-Y., Tachi-Duprat, M., Ihewulezi, C., Devotta, A., Saint-Jeannet, J.-P., 2022. The core splicing factors EFTUD2, SNRPB and TXNL4A are essential for neural crest and craniofacial development. J. Dev. Biol. 10 (3), 29.

Pegoraro, C., Monsoro-Burq, A.H., 2013. Signaling and transcriptional regulation in neural crest specification and migration: lessons from Xenopus embryos. Wiley Interdisc. Rev.: Dev. Biol. 2, 247–259.
Piekarski, N., Gross, J.B., Hanken, J., 2014. Evolutionary innovation and conservation in the embryonic derivation of the vertebrate skull. Nat. Commun. 5, 5661.
Plouhinec, J.-L., Medina-Ruiz, S., Borday, C., Bernard, E., Vert, J.-P., Eisen, M.B., Harland, R.M., Monsoro-Burq, A.H., 2017. A molecular atlas of the developing ectoderm defines neural, neural crest, placode, and nonneural progenitor identity in vertebrates. PLoS Biol. 15 (10), e2004045.
Prasad, M.S., Sauka-Spengler, T., LaBonne, C., 2012. Induction of the neural crest state: control of stem cell attributes by gene regulatory, post-transcriptional and epigenetic interactions. Dev. Biol. 366, 10–21.
Rao, A., LaBonne, C., 2018. Histone deacetylase activity has an essential role in establishing and maintaining the vertebrate neural crest. Development 145 (15), dev163386.
Ring, D.B., Johnson, K.W., Henriksen, E.J., Nuss, J.M., Goff, D., Kinnick, T.R., Ma, S.T., Reeder, J.W., Samuels, I., Slabiak, T., 2003. Selective glycogen synthase kinase 3 inhibitors potentiate insulin activation of glucose transport and utilization in vitro and in vivo. Diabetes 52, 588–595.
Sanvitale, C.E., Kerr, G., Chaikuad, A., Ramel, M.-C., Mohedas, A.H., Reichert, S., Wang, Y., Triffitt, J.T., Cuny, G.D., Yu, P.B., 2013. A new class of small molecule inhibitor of BMP signaling. PLoS One 8 (4), e62721.
Sato, T., Sasai, N., Sasai, Y., 2005. Neural crest determination by co-activation of Pax3 and Zic1 genes in Xenopus ectoderm. Development 132, 2355–2363.
Scarpa, E., Szabo, A., Bibonne, A., Theveneau, E., Parsons, M., Mayor, R., 2015. Cadherin switch during EMT in neural crest cells leads to contact inhibition of locomotion via repolarization of forces. Dev. Cell 34, 421–434.
Scerbo, P., Monsoro-Burq, A.H., 2020. The vertebrate-specific VENTX/NANOG gene empowers neural crest with ectomesenchyme potential. Sci. Adv. 6 (18), eaaz1469.
Schock, E.N., LaBonne, C., 2020. Sorting sox: diverse roles for sox transcription factors during neural crest and craniofacial development. Front. Physiol. 11, 606889.
Schock, E.N., York, J.R., LaBonne, C., 2023. The developmental and evolutionary origins of cellular pluripotency in the vertebrate neural crest. Semin. Cell Dev. Biol. 138, 36–44.
Schwenty-Lara, J., Nehl, D., Borchers, A., 2020. The histone methyltransferase KMT2D, mutated in Kabuki syndrome patients, is required for neural crest cell formation and migration. Hum. Mol. Genet. 29, 305–319.
Session, A.M., Uno, Y., Kwon, T., Chapman, J.A., Toyoda, A., Takahashi, S., Fukui, A., Hikosaka, A., Suzuki, A., Kondo, M., 2016. Genome evolution in the allotetraploid frog Xenopus laevis. Nature 538, 336–343.
Shah, A.M., Krohn, P., Baxi, A.B., Tavares, A.L., Sullivan, C.H., Chillakuru, Y.R., Majumdar, H.D., Neilson, K.M., Moody, S.A., 2020. Six 1 proteins with human branchio-oto-renal mutations differentially affect cranial gene expression and otic development. Dis. Models Mech. 13 (3), dmm043489.
Takahashi, M., Tamura, K., Buscher, D., Masuya, H., Yonei-Tamura, S., Matsumoto, K., Naitoh-Matsuo, M., Takeuchi, J., Ogura, K., Shiroishi, T., 1998. The role of Alx-4 in the establishment of anteroposterior polarity during vertebrate limb development. Development 125, 4417–4425.
Timberlake, A.T., Griffin, C., Heike, C.L., Hing, A.V., Cunningham, M.L., Chitayat, D., Davis, M.R., Doust, S.J., Drake, A.F., Duenas-Roque, M.M., 2021. Haploinsufficiency of SF3B2 causes craniofacial microsomia. Nat. Commun. 12, 4680.
Vega-Lopez, G.A., Cerrizuela, S., Tribulo, C., Aybar, M.J., 2018. Neurocristopathies: new insights 150 years after the neural crest discovery. Dev. Biol. 444, S110–S143.
Wühr, M., Freeman Jr., R.M., Presler, M., Horb, M.E., Peshkin, L., Gygi, S.P., Kirschner, M.W., 2014. Deep proteomics of the Xenopus laevis egg using an mRNA-derived reference database. Curr. Biol. 24, 1467–1475.
Wyatt, B.H., Raymond, T.O., Lansdon, L.A., Darbro, B.W., Murray, J.C., Manak, J.R., Dickinson, A.J., 2020. Using an aquatic model, Xenopus laevis, to uncover the role of chromodomain 1 in craniofacial disorders. Genesis 59 (1–2), e23394.
Yanai, I., Peshkin, L., Jorgensen, P., Kirschner, M.W., 2011. Mapping gene expression in two Xenopus species: evolutionary constraints and developmental flexibility. Dev. Cell 20, 483–496.
York, J.R., McCauley, D.W., 2020. The origin and evolution of neural crest cells. Open Biol. 10 (1), 190285.
York, J.R., Yuan, T., McCauley, D.W., 2020. Evolutionary and developmental associations of neural crest and placodes in the vertebrate head: insights from jawless vertebrates. Front. Physiol. 11, 986.
Zalc, A., Sinha, R., Gulati, G.S., Wesche, D.J., Daszczuk, P., Swigut, T., Weissman, I.L., Wysocka, J., 2021. Reactivation of the pluripotency program precedes formation of the cranial neural crest. Science 371 (6529).